

# SIGNIFICANCE OF MHD EFFECTS IN STELLARATOR CONFINEMENT

A. WELLER,\*† S. SAKAKIBARA,‡ K. Y. WATANABE,‡ K. TOI,‡ J. GEIGER,†  
M. C. ZARNSTORFF,§ S. R. HUDSON,§ A. REIMAN,§ A. WERNER,† C. NÜHRENBERG,†  
S. OHDACHI,‡ Y. SUZUKI,‡ H. YAMADA,‡ W7-AS TEAM,† and LHD TEAM‡

†Max-Planck-Institut für Plasmaphysik, EURATOM-IPP Association, D-17491 Greifswald, Germany

‡National Institute for Fusion Science, Toki 509-5292, Japan

§Princeton Plasma Physics Laboratory, Princeton, NJ 08543

Received October 27, 2005

Accepted for Publication January 13, 2006

*Substantial progress has been achieved in raising the plasma beta in stellarators and helical systems by high-power neutral beam heating, approaching reactor-relevant values. The achievement of high-beta operation is closely linked with configuration effects on the confinement and with magnetohydrodynamic (MHD) stability.*

*The magnetic configurations of the Wendelstein 7-AS (W7-AS) stellarator and of the Large Helical Device (LHD) and their optimization for high-beta operation within the flexibility of the devices are characterized. A comparative description of the accessible operational regimes in W7-AS and LHD is given. The finite-beta effects on the flux surfaces depend on the degree of configuration optimization. In particular, a large Shafranov shift is accompanied by formation of islands and stochastic field regions as found by numerical equilibrium studies. However, the observed pressure gradients indicate some mitigation of the effects on the plasma confinement, presumably because of the high collisionality of high-*

*beta plasmas and island healing effects (LHD). As far as operational limits by pressure-driven MHD instabilities are concerned, only weak confinement degradation effects are usually observed, even in linearly unstable regimes.*

*The impact of the results concerning high-beta operation in W7-AS and LHD on the future stellarator program will be discussed, including the relationship to tokamak research. Some of the future key issues appear to be the following: the control of the magnetic configuration (including toroidal current control), the modification of confinement and MHD properties toward the low-collisional regime, and the compatibility of high-beta regimes with power and particle exhaust requirements to achieve steady-state operation.*

**KEYWORDS:** stellarator, confinement, magnetohydrodynamics

## I. INTRODUCTION

The development of a viable and economic fusion energy source is the basic goal of the international fusion research program. At present, the tokamak is most advanced, and the achievement of a burning plasma state in the International Thermonuclear Experimental Reactor<sup>1</sup> (ITER) will be a crucial milestone in future fusion research based on magnetic confinement. The considerable progress achieved in stellarators and helical systems appears to provide an even more attractive alternative for a

fusion reactor. Stellarators and helical systems have the inherent potential of stable, disruption-free, steady-state plasma confinement without the necessity for either current drive, control of plasma position and of edge flux surface topology, or for active feedback and near-plasma conducting structures to stabilize instabilities. A variety of different magnetic configurations has been realized or proposed. The bumpiness of the nonaxisymmetric magnetic field in stellarators determines the confinement and magnetohydrodynamic (MHD) properties that can be optimized by proper three-dimensional (3-D) shaping of the plasma boundary. "Reverse engineering" has constituted an innovative approach to meet desired physics

\*E-mail: arthur.weller@ipp.mpg.de

targets, as realized in the Wendelstein 7-X (W7-X) (Helias concept)<sup>2</sup> and the compact quasi-symmetric stellarator design [e.g., National Compact Stellarator Experiment (NCSX) and Helically Symmetric Experiment (HSX)] (Refs. 3, 4, and 5). On the other hand, configuration optimization within the device flexibility has led to considerably improved plasma confinement in the Large Helical Device (LHD) (Heliotron device) without compromising stability significantly.<sup>6,7</sup> This shows that a sufficient degree of flexibility in present and future stellarator experiments is required in order to quantify trade-offs between desired properties.

The economic use of fusion power requires volume-averaged plasma beta values in the order of  $\langle\beta\rangle \approx 5\%$  (here, beta defined by  $\langle\beta\rangle = 2\mu_0\langle p/B^2\rangle$  is the volume-averaged plasma pressure normalized to the magnetic field pressure). High-beta operation is closely related to MHD equilibrium and stability issues. In this paper, we review the experimental progress of achieving relevant plasma beta in stellarators based on work conducted at Wendelstein 7-AS (W7-AS) (Refs. 8 and 9) and at LHD (Ref. 6) (Sec. II). In Sec. II.A, the two devices and their basic configuration properties are characterized. Section II.B describes the optimization of the experimental methods to maximize the achievable plasma beta. Confinement properties and the operational ranges are discussed and compared. A main concern is finite-beta effects on the magnetic configuration. Section II.C deals with equilibrium aspects and associated beta limits. MHD stability properties and the relevance of MHD instabilities as regards stable high-beta confinement are discussed in Sec. II.D. Section III is devoted to discussing the impact of the results on the future stellarator program and remaining issues.

## II. PROGRESS OF HIGH-BETA OPERATION IN STELLARATORS/HELICAL SYSTEMS

Before start of LHD operation, beta values in the 1.5 to 2% range have been reported by several stellarator experiments including Heliotron-E (Ref. 10), the Advanced Torsatron Facility (ATF) (Ref. 11), the Compact Helical System (CHS) (Ref. 12), and W7-AS. Here, we are focusing on more recent results from W7-AS and LHD. A major concern is to compare the results in order to achieve a more comprehensive understanding of the underlying physics of beta-induced MHD effects in 3-D confinement systems.

### II.A. W7-AS and LHD Configurations

Wendelstein 7-AS (Refs. 13 and 14) is a medium-sized stellarator ( $R = 2$  m;  $a \leq 0.18$  m) operated until mid-2002. The five-period magnetic field is partially optimized with respect to MHD properties (reduced Pfirsch-Schlüter currents) and neoclassical transport by 3-D shaping. The field ( $B \leq 2.5$  T) is generated by a system

of 45 nonplanar modular coils providing a low-shear rotational transform of  $t_{vac} \approx 0.4$ . The vacuum rotational transform can be varied in the range  $0.25 \leq t_{vac} \leq 0.65$  by an extra set of ten planar toroidal field coils. Additionally, poloidal field coils allow one to adjust the horizontal plasma position. Current drive and current control are accomplished by an ohmic transformer. Since 2000, W7-AS has been equipped with a modular island divertor system<sup>15</sup> including a set of ten in-vessel coils for controlling the width of edge islands by resonant field perturbations  $B_{5m}$ . High-beta plasmas are heated by almost tangential neutral beam injection (NBI) with beam energies of 50 to 55 keV yielding absorbed heating powers of  $P_{NBI} \leq 3.2$  MW. The heating efficiency decreases toward lower fields restricting high-beta operation to  $B \geq 0.7$  T.

The LHD (Ref. 16) is the largest existing heliotron-type helical device ( $R = 3.9$  m;  $a \leq 0.65$  m). The magnetic field of ten field periods ( $B \leq 3$  T) is produced by a pair of superconducting helical windings (heliotron-type configuration). Three sets of poloidal field coils are used to change the axis position of the vacuum configuration in the range  $R_{ax} = 3.4$  to 4.1 m and for plasma shaping. The profile of the vacuum rotational transform in the LHD features much higher shear compared with W7-AS. The central and edge values are in the range  $t_{vac}(0) \geq 0.35$  and  $t_{vac}(a) \leq 1.5$ , respectively. The rotational transform can be varied by changing the center of the current in the helical coils. In addition, a set of external saddle coils allows one to drive an  $n/m = 1/1$  magnetic island at the plasma edge, which can be utilized for local island divertor (LID) operation and island studies.<sup>6,17</sup> The heating power of  $P_{NBI} \leq 9.5$  MW (absorbed) is provided by three tangential beam lines using negative ions with beam energies of 150 to 180 keV.

The basic configuration parameters of W7-AS and LHD in terms of the magnetic shear and the magnetic well are compared in Fig. 1. The profiles were calculated as a function of beta with the VMEC 3-D equilibrium code<sup>18</sup> using model pressure profiles. W7-AS is characterized by low shear, allowing one to avoid low-order iota resonances, and a magnetic well over the entire plasma (besides at very low beta due to large inward shift). In LHD, the shear is much larger, particularly in the edge region. The inwardly shifted vacuum configuration ( $R_{ax} = 3.6$  m) has no magnetic well, but it develops in the center and expands as beta is raised. The plasma edge remains in a magnetic hill region.

### II.B. High-Beta Operation in W7-AS and LHD: Global Confinement and Operational Range

The experimental conditions in both devices had to be optimized to develop beta to the maximum. In W7-AS, several measures and related effects have resulted in quiescent quasi-stationary discharges with beta up to  $\langle\beta\rangle = 3.4\%$ . First, high- $t$  configurations with higher

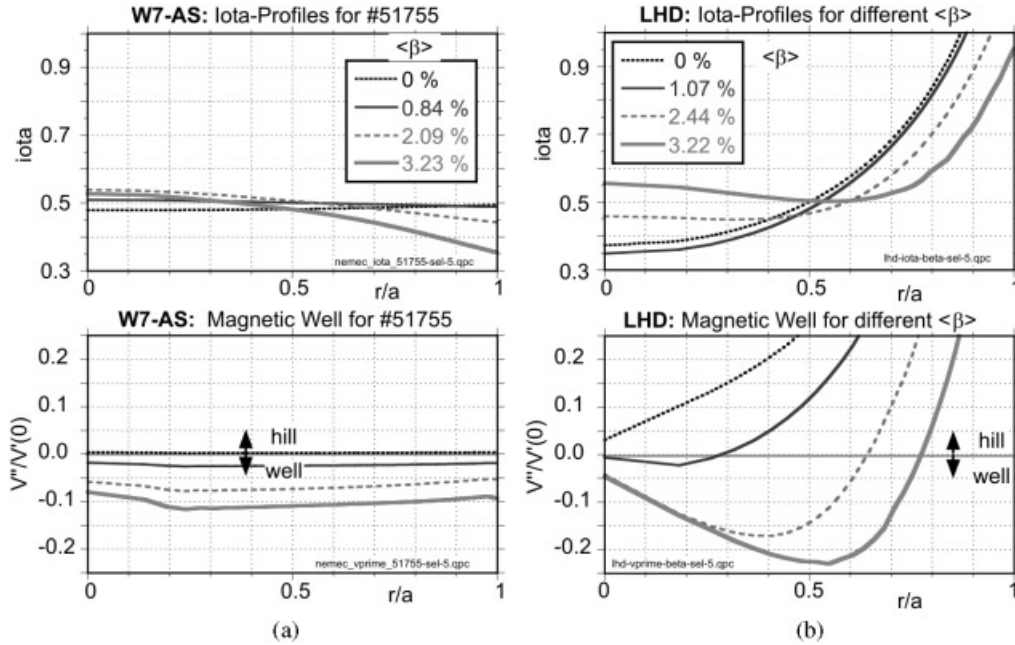


Fig. 1. Finite-beta effects on radial profiles of the rotational transform  $\iota$  and the magnetic well depth  $V''(\rho)/V'(0)$  ( $V$ : volume,  $\rho = r/a$ ) calculated by the VMEC code for (a) W7-AS and (b) LHD. The vacuum configurations are inwardly shifted ( $R_{ax} = 3.6$  m in LHD).

equilibrium limit (see Sec. II.C) could be exploited. Maximizing of the plasma volume, and hence of the global confinement, was achieved by suppressing the edge islands with the divertor control coils. Second, controlling the plasma position in the high-beta phase and limiting the plasma by the divertor structure allowed one to maintain high-density H-mode (HDH) confinement.<sup>19</sup> Third, the NBI heating efficiency at low magnetic field could significantly be raised by changing the NBI into an all-conjecting system.

In LHD, a key element is to choose an inwardly shifted configuration ( $R_{ax} = 3.6$  m) that provides significantly enhanced confinement even in the high-collisional regime.<sup>7,20</sup> Second, configurations with minimum Shafranov shift were selected in order to exploit the full NBI power by keeping the plasma center as closely as possible aligned with the radius of tangency of the neutral beams  $R_{T,NBI} = 3.65$  to 3.7 m. This could be achieved by decreasing the coil current pitch parameter ( $\gamma = 1.254 \rightarrow 1.22$ ) resulting in a larger aspect ratio ( $A_p \equiv R/a \approx 5.8 \rightarrow 6.3$ ) and higher central rotational transform, and hence in a reduced Shafranov shift. Discharges with beta up to  $\langle\beta\rangle = 4.2\%$  could be realized.

A summary of the achieved beta in W7-AS and LHD is shown in Fig. 2. The W7-AS database contains a selected set of cases, for which an equilibrium analysis with VMEC was available. The LHD database contains an approximate analysis of all shots of the last two experimental campaigns (seventh and eighth) with  $\langle\beta\rangle > 1.5\%$ . A more accurate evaluation requires a more

elaborate equilibrium analysis. The diamagnetic beta values in LHD contain a significant fraction of fast ions;  $\langle\beta\rangle_{beam}$  is estimated to range up to  $\sim 1.5\%$ . In both experiments, the flattop time (defined as a time interval for which beta does not change by  $> 10\%$ ) around the time of analysis ranges up to approximately 100 energy confinement times.

The global energy confinement times in both experiments are above the ISS95 scaling,<sup>21</sup> as shown in Fig. 3. In LHD, a progressive degradation of the confinement toward higher beta is found in the H-factors. This may be caused by a combination of three effects: the increasing violation of MHD stability (see Sec. II.D), the formation of a stochastic field region (see Sec. II.C), and a less beneficial confinement scaling at high densities ( $\nu^*$ ) (Refs. 6 and 22).

If the rotational transform (at  $\rho \equiv r/a = 2/3$ , representing an estimate of the volume average) is formally replaced by an equivalent toroidal current by equating  $t_{2/3} \approx 1/q_{95} \propto I_{eq}$  (Refs. 1, 8, and 23), the confinement can be compared with tokamak scaling laws. Using the mean elongation of the configurations ( $\kappa \approx 2$  for W7-AS;  $\kappa \approx 1$  for LHD) yields reasonable agreement of the W7-AS and LHD data with ITER ELMy H-Mode scaling [IPB98(y,2) (Refs. 1 and 24)].

The accessible density range differs significantly in W7-AS compared to LHD due to the different heating power densities and magnetic field range. In W7-AS, the plasma volume is  $\sim 1$  m<sup>3</sup>, and the maximum beta is achieved with  $B = 0.8 \dots 0.9$  T compared to  $\sim 30$  m<sup>-3</sup>

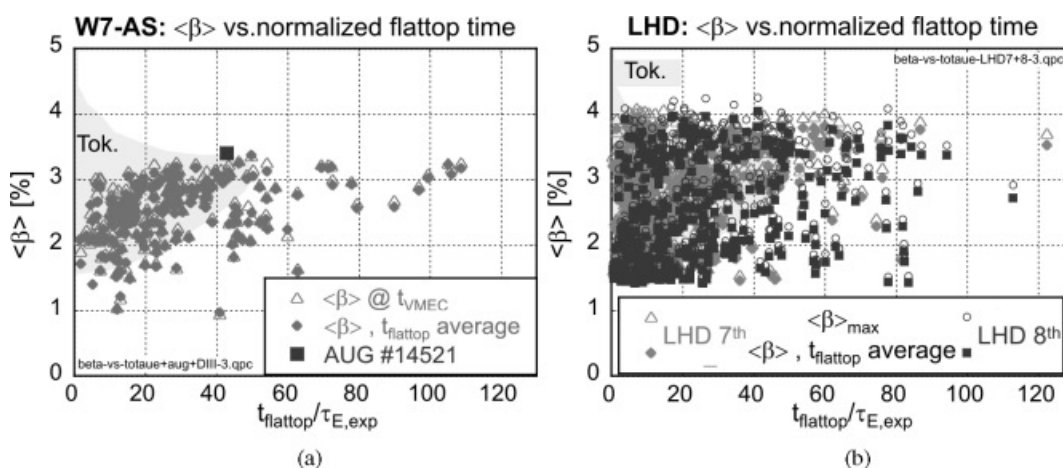


Fig. 2. High-beta databases of (a) W7-AS and (b) LHD (seventh and eighth campaigns). Volume-averaged beta values are given as a function of the flattop time normalized to the confinement time. The open symbols refer to the time in the discharge at which the VMEC analysis was performed. The solid symbols represent time averages during the flattop. In addition, the typical range of tokamak data is indicated by the shaded area.

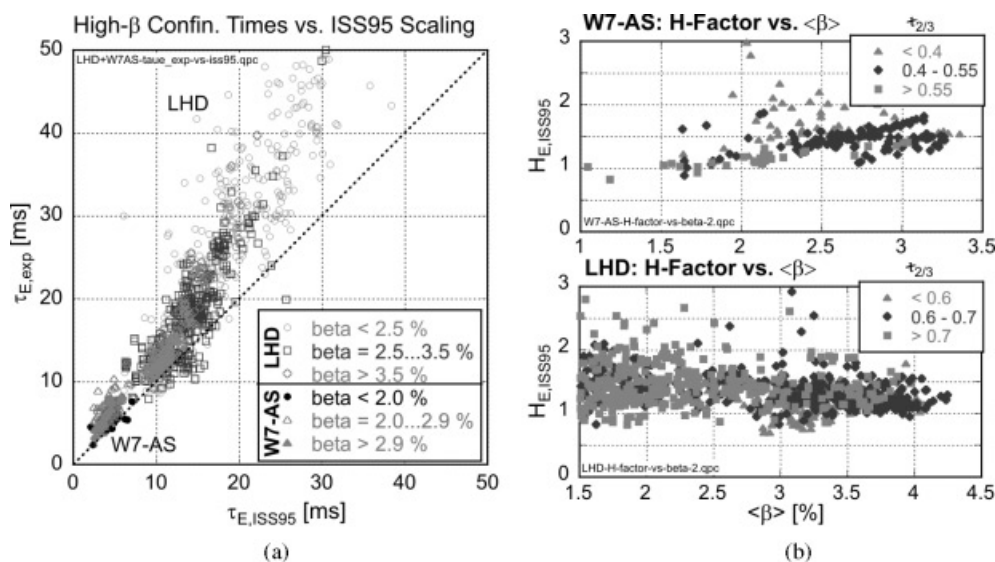


Fig. 3. (a) Comparison of experimental energy confinement times with the ISS95 scaling for the same W7-AS and LHD high-beta databases as used in Fig. 2. The H-factors (enhancement  $\tau_{E,\text{exp}}/\tau_{E,\text{ISS95}}$ ) are given in (b).

and  $B = 0.45 \dots 0.5$  T in LHD. Therefore, a much higher density limit (derived from power balance considerations<sup>25,26</sup>) is predicted for W7-AS. In Fig. 4, densities of the W7-AS and LHD high-beta databases are compared with the Sudo limit:

$$\bar{n}_{\text{Sudo-DL}} \equiv 1.11 \cdot (P \cdot B / V)^{0.5} \quad [10^{20} \text{ m}^{-3}] .$$

### II.C. Finite-Beta Effects on Equilibrium Topology and Confinement

The most prominent effect of finite-beta in toroidal magnetic confinement is the Shafranov shift, which leads

to a mainly horizontal shift of the magnetic surfaces due to the parallel component of the equilibrium current (Pfirsch-Schlüter current).<sup>27</sup> In a low-beta, large-aspect-ratio approximation, the Shafranov shift is

$$\frac{\Delta}{a} \approx A_p \frac{\langle\beta\rangle}{2t^2} \quad (A_p = R/a)$$

for a classical stellarator, whereas a reduction by approximately one-half is found (as expected) in W7-AS (Ref. 8). In LHD,  $t \propto A_p$ , and hence,  $\Delta/a \propto 1/A_p$ . A rough estimate of an equilibrium beta limit follows from the condition

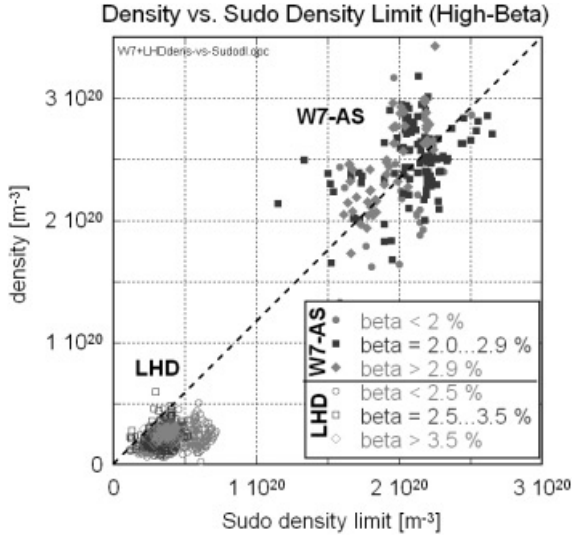


Fig. 4. Densities for same W7-AS and LHD high-beta databases as used in Fig. 2b compared with Sudo density limit<sup>25</sup> (dashed line).

$\Delta/a = \frac{1}{2}$ , which is considered to lead to the destruction of the equilibrium surfaces. The strong dependence on the rotational transform is reflected in the W7-AS and LHD database analysis as presented in Fig. 5. The data in both experiments suggest that low rotational transform (which is associated with a lower equilibrium limit) imposes a limit on the  $\langle\beta\rangle$  values that can be achieved.

The beta-induced axis shift has been measured in W7-AS by X-ray tomography<sup>8</sup> and in LHD using Thom-

son scattering data and tangential X-ray imaging.<sup>28,29</sup> In LHD, also the shift of the last closed flux surface (LCFS) could be determined. The experimental data are in reasonable agreement with free boundary equilibrium code calculations [VMEC in W7-AS; HINT (Ref. 30) in LHD]. The predicted and measured shifts in W7-AS and LHD are compared in Fig. 6 for typical high-beta configurations. The LCFS shift in LHD is relatively small due to high edge rotational transform. The normalized shift of the axis relative to the center of the LCFS ( $\Delta/a$ , Shafranov shift) is comparable in these particular W7-AS and LHD cases. The slope of  $\Delta/a$  is a little more flat in W7-AS, but the absolute value is slightly higher due to an opposite offset of  $\Delta/a$  compared to LHD. In both cases, the Shafranov shift remains clearly below the critical value  $\Delta/a = \frac{1}{2}$ . A deeper insight into the equilibrium limit is gained from advanced 3-D equilibrium code calculations without the premise of nested flux surfaces.

Figure 7 compares the flux surface topology of high-beta equilibria as obtained from the PIES code<sup>31</sup> (W7-AS case) and the HINT code<sup>30</sup> (LHD case). Both PIES and HINT predict a progressive loss of good flux surfaces with increasing plasma pressure. The significant degree of surface destruction shown in Fig. 7 corresponds to equilibria close to the maximum achieved beta values. The cause of the generation of islands and stochastic regions in finite-beta equilibria are resonant field harmonics of the vacuum field and resonant field perturbations produced by the Pfirsch-Schlüter currents. Therefore, the widths of the perturbations depend on the plasma pressure. The effects could be mitigated to some extent in W7-AS by changing the perturbed field spectrum using the divertor control coils.<sup>9</sup>

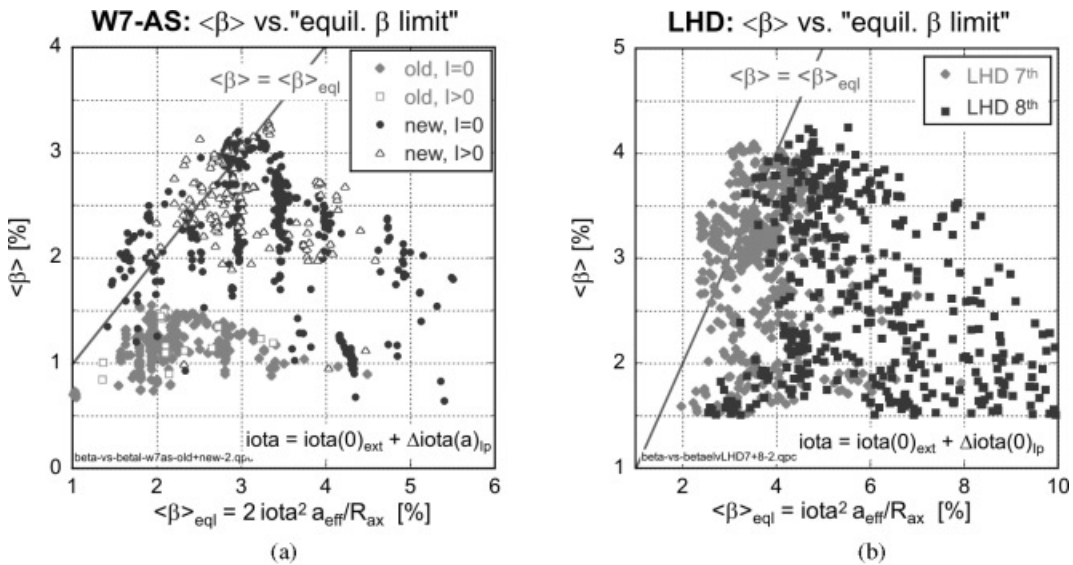


Fig. 5. Achieved  $\langle\beta\rangle$  in W7-AS and LHD plotted versus  $c\tau^2/A_p \equiv \langle\beta\rangle_{eql}$  as an estimate of an equilibrium beta limit corresponding to  $\Delta/a = \frac{1}{2}$  ( $c = 2$  for W7-AS;  $c = 1$  for LHD). The solid line represents  $\langle\beta\rangle = \langle\beta\rangle_{eql}$ .

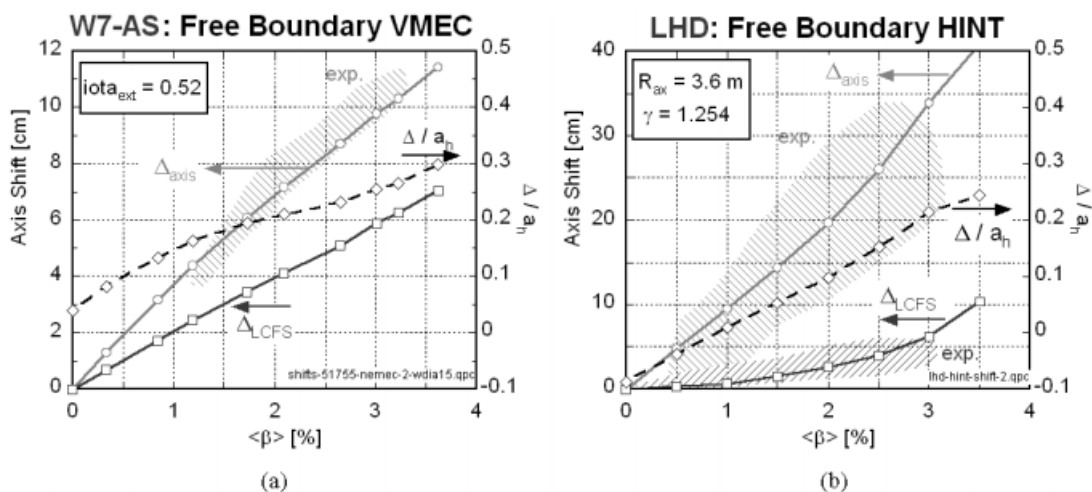


Fig. 6. (a) VMEC (W7-AS) and (b) HINT (LHD) free boundary predictions of beta-induced horizontal shifts of the plasma axis (circles), the LCFS (squares), and their difference (Shafranov shift normalized to horizontal plasma radius  $a_h$ , black dashed line, right scales). The shaded areas represent the range of available experimental data.

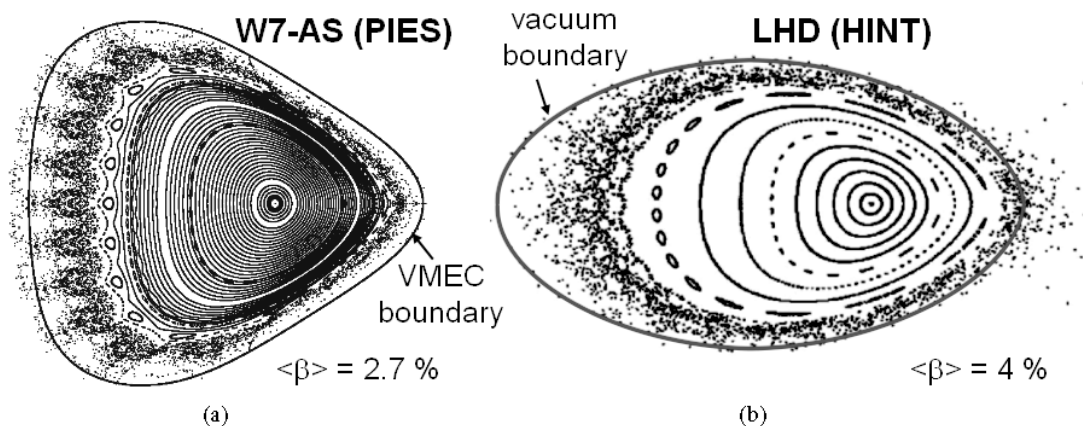


Fig. 7. Free boundary high-beta equilibria as calculated (a) for W7-AS with PIES and (b) for LHD with HINT. A large fraction of flux surfaces is predicted to be degraded by island formation and generation of stochastic field regions.

Surprisingly, the impact of the predicted stochastic field regions on the experimentally observed pressure profiles is only moderate. In both experiments, significant pressure gradients are found in such regions.<sup>9,32,33</sup> Therefore, islands and stochastic field regions may not be destroyed to the extent predicted by static equilibrium calculations. Actually, healing of an externally driven  $m/n = 1/1$  island has been observed in LHD (Refs. 17, 34, and 35). The observation of a critical island size below which the island is annihilated suggests a stabilization mechanism closely related to neoclassical tearing mode (NTM) physics.<sup>17,36</sup> The expected dependencies of the island size in LHD on beta and collisionality have been found qualitatively by using an axisymmetric neoclassical bootstrap current model. A proper 3-D bootstrap current model is required for quantitative understand-

ing.<sup>17</sup> Since the plasma in the present high-beta experiments is in a relatively high-collisionality regime (in particular in W7-AS), effects due to an increased ratio of perpendicular-to-parallel transport may also contribute to reduce the effect of perturbed flux surfaces on the pressure profiles. In any case, indications of enhanced radial transport by parallel conduction in regions of relatively short radial connection lengths are found both in LHD (Ref. 17) and W7-AS (Ref. 37).

#### II.D. MHD Stability, Impact of MHD Modes on High-Beta Plasmas

In tokamaks, the operational range of beta is clearly limited by MHD instabilities such as NTMs, disruptions, resistive wall modes, or edge-localized modes when

theoretical stability limits are approached. Although the same underlying physics has to be expected, the MHD effects in stellarators seem to be somewhat different. The linear ideal MHD stability properties predicted for W7-AS and LHD high-beta configurations (as introduced in Sec. II.A) are evaluated as a guideline for comparisons with experimental data. Close agreement cannot be expected without using more sophisticated MHD models including nonlinear and nonideal effects. Also, accurate reconstruction of the equilibrium from experimental data is required to check the agreement with theory since the stability can sensitively depend on details of the pressure and iota profiles. A big issue is the treatment of stochastic regions and the determination of the plasma boundary (see end of Sec. II.C). A suitable theoretical approach could be to assume averaged flux surfaces in stochastic magnetic field regions.<sup>38</sup>

In Fig. 8, the local ideal interchange stability in terms of Mercier stability diagrams is compared for optimum high-beta configurations in W7-AS and LHD using fixed model pressure profiles. The configuration of W7-AS is predicted to be unstable below  $\langle\beta\rangle = 1.5\%$  across the whole plasma radius due to the flat shear and the transition from the magnetic hill in the vacuum configuration to a magnetic well at finite beta (see Fig. 1a). The edge remains unstable because the pressure gradient rises toward the plasma boundary (available equilibrium reconstructions were made with parabolic pressure profiles). Low-order rational surfaces at  $\iota = \frac{1}{2}$  and  $\iota = \frac{1}{3}$  appear during the formation of a broad stable region along with increased shear, moving inward as pressure and shear are further increased. The unstable region in the LHD configuration with axis position  $R_{ax} = 3.75$  m is rather small because of a marginal magnetic hill region in the center and effective shear stabilization. However, as already mentioned in Sec. II.B, the confinement is unfavorable. The inwardly shifted configuration with  $R_{ax} = 3.6$  m has

good confinement properties, but the unstable region is much wider in radius and extended over a broader range in beta because of an increased magnetic hill region (the dashed lines indicate the separation between the magnetic hill and the magnetic well regions).<sup>39</sup>

The path toward high-beta plasmas has to traverse regions predicted to be unstable with respect to ideal interchange modes and global (low- $n$ ) ideal modes. The violation of the Mercier stability criterion, however, does not inhibit the access to higher beta in both experiments by using higher heating power. Global low- $n$  interchange modes are found in W7-AS (Refs. 8, 9, and 10) and LHD (Refs. 41 through 45), mostly consistent with predictions based on the linear MHD stability theory. However, in most cases the observed modes saturate on a harmless level. Therefore, the low- $n$  linear stability threshold significantly underestimates the achievable beta. Typical behavior of high-beta discharges in W7-AS with respect to MHD modes is shown in Fig. 9. The range of beta where the pressure-driven  $m = 2$  global mode is seen by magnetic diagnostics and X-ray tomography is consistent with predictions by the ideal global mode analysis with the CAS3D code.<sup>46,47</sup> At the maximum  $\beta$ , the discharges are very quiescent consistent with linear stability prediction for low- $n$  interchange and high- $n$  ideal ballooning modes.

Extended MHD stability studies have been performed in LHD. In particular, experimentally determined beta gradients are compared with linear stability thresholds and with observed mode amplitudes.<sup>28,33,48,49</sup> Figure 10 contains a local analysis for a surface close to the plasma periphery and for a surface in the plasma core. In spite of mode activity in the Mercier unstable region, the beta gradients can be increased. However, unstable low- $n$  interchange modes with growth rates  $\gamma/\omega_A \geq 10^{-2}$  ( $\omega_A = v_A/R$ ), corresponding to a radial width of the modes of  $\delta/a \sim 5\%$ , seem to be relevant and limit the achievable beta gradients in the unstable region. In the stability

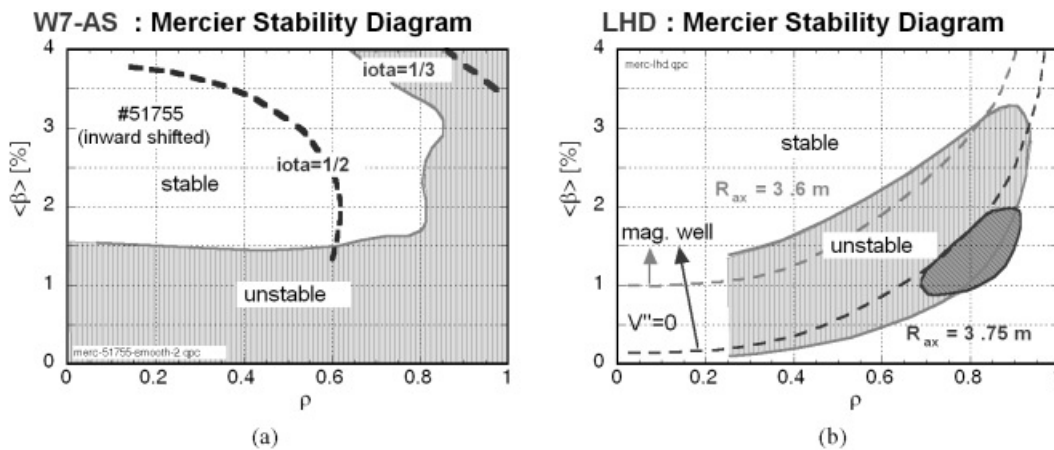


Fig. 8. Mercier stability diagrams for (a) W7-AS and (b) LHD configurations. The W7-AS and LHD ( $R_{ax} = 3.6$  m) configurations are inwardly shifted and less stable.

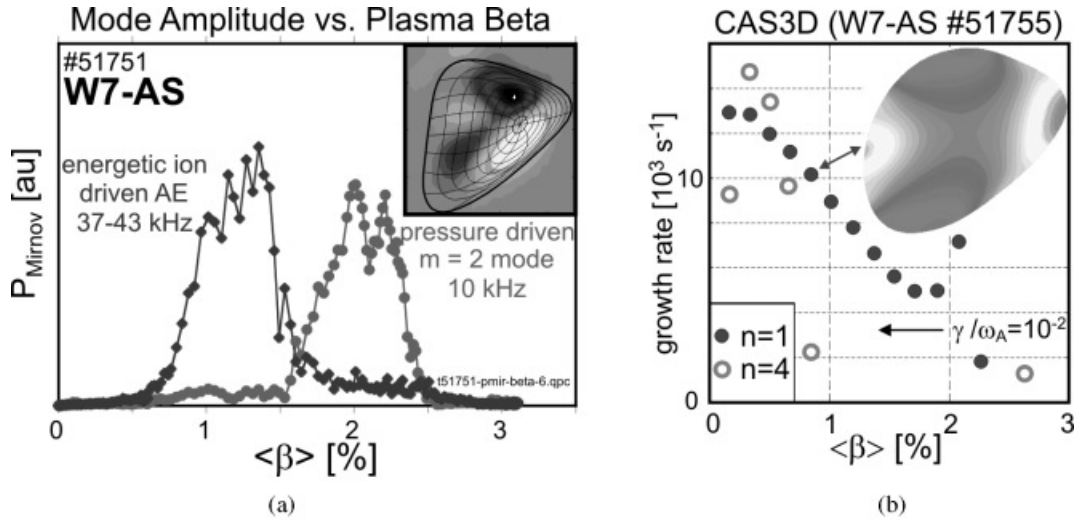


Fig. 9. Mode amplitudes in W7-AS depending on beta. The observed  $m/n = 2/1$  pressure-driven mode [(a), inset: X-ray tomogram] disappears above  $\langle\beta\rangle = 2.5\%$  in agreement with vanishing growth rates of global ideal modes as predicted by CAS3D (b).

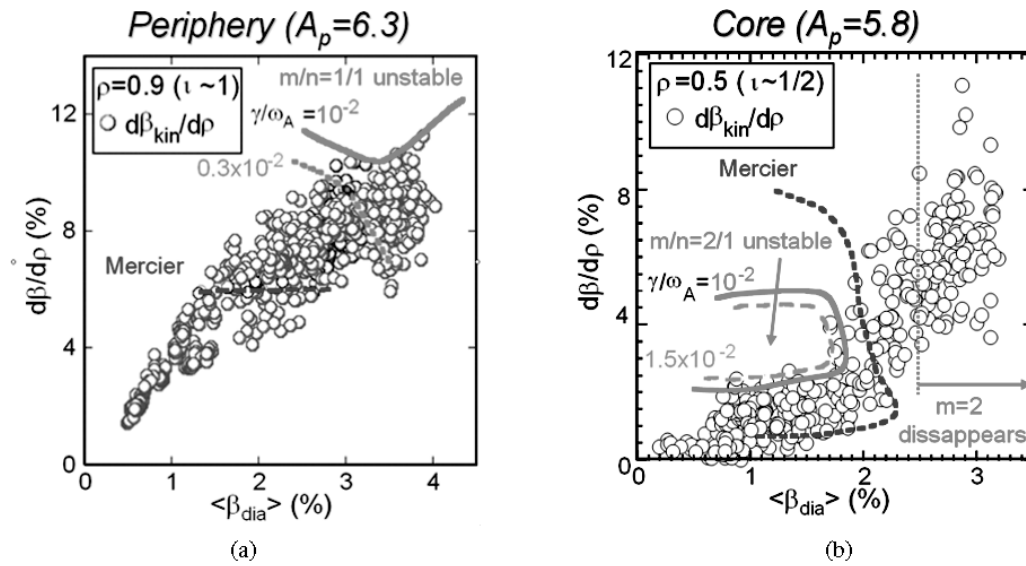


Fig. 10. Observed gradients of beta in LHD (a) at the plasma periphery ( $\rho = 0.9$ ) and (b) in the core ( $\rho = 0.5$ ) plotted against  $\langle\beta\rangle$ . Stability thresholds for the Mercier stability are significantly violated in experiment. The threshold for low- $n$  ideal interchange modes with growth rates  $\gamma/\omega_A = 10^{-2}$  is not exceeded in experiment. The presence of observed MHD modes correlates with the Mercier unstable region.

analysis, effects due to bootstrap and Ohkawa currents ( $\leq 25$  kA/T) were neglected. This is a reasonable assumption at the plasma edge (Fig. 10a) since the increment of iota due to the currents is  $< 0.03$ . However, in the plasma core (Fig. 10b) the currentless assumption corresponds to an upper stability limit since the current in the selected co-NBI and balanced NBI cases reduces the ideal interchange stability via the change of the equilib-

rium.<sup>50</sup> The low- $n$  ideal MHD unstable boundaries are derived from calculations with the TERPSICHORE 3-D MHD stability code<sup>51</sup> using various beta values and pressure profiles.<sup>49</sup> High- $n$  ideal ballooning modes are expected to have very similar stability thresholds. Core MHD is effectively stabilized by the pressure-induced formation and progressive deepening of a magnetic well. This self-stabilization mechanism is similar as in W7-AS.

In contrast, the ideal stability at the plasma edge relies entirely on magnetic shear. The amplitudes of observed edge MHD modes typically increase with rising beta. Therefore, the edge stability is crucial for maintaining broad pressure profiles with large edge gradients, in particular, if shear stabilization is annihilated by resistive effects.

The favorable LHD configurations for achieving maximum beta (reduced gamma parameter, increased aspect ratio, and central rotational transform  $R_{ax} = 3.6$  m) are more unstable because of lower shear and restricted magnetic well formation (reduced Shafranov shift). The  $t = 1$  surface is located farther inward, in particular, when a significant plasma current (mostly Ohkawa current) increases the external rotational transform. In this case the ideal  $m/n = 1/1$  is unstable at low beta, and strong activities including internal disruptions in the core region are found. An example of a large MHD-induced collapse is presented in Fig. 11. Internal disruptions are also seen at other rational surfaces ( $t = \frac{1}{2}, \frac{1}{3}, \text{etc.}$ ) if present in the plasma core. But, the effect on the confinement is much larger in the case with  $t = 1$  (Ref. 52).

Indications of resistive MHD effects have been found in W7-AS and LHD. The magnetic Reynolds number  $S = \tau_{res}/\tau_A$  for high-beta conditions is typical  $S \sim 10^5$  in W7-AS and  $S \sim 10^6$  in LHD. Fast thermal collapses occur in W7-AS high-beta cases in correlation with decreased electron temperature and low rotational transform.<sup>53</sup> The fast collapse of the plasma energy ( $\sim 100 \mu\text{s}$ ) is accompanied by a magnetic spike of the same duration. The observed scaling of this instability with plasma and configuration parameters is consistent with that of resistive ballooning modes, if linear growth rates<sup>54</sup> are used as a measure of the expected mode activity:  $\gamma \approx (\langle\beta\rangle/\langle\beta\rangle_c)\eta k^2/\mu_0 \propto (\langle\beta\rangle/t^2)T_e^{-3/2}$ , where  $\langle\beta\rangle_c \propto t^2$  is the ideal ballooning limit that roughly coincides with the

equilibrium beta limit. The linear dependence of  $\gamma$  on  $\eta$  results from the so-called resistive pressure convection limit model with the additional conditions of low growth rates and sufficiently low resistivity.<sup>55–57</sup> Only qualitative considerations have been made about the validity of these conditions. Since the resistivity of high-beta plasmas in LHD is much lower than in W7-AS, the stabilizing effect by plasma compression is more important in LHD, and the  $\gamma \sim \eta^{1/3}$  regime can then be recovered. Figure 12 shows a W7-AS data set containing the high-beta database including all cases where fast collapses were observed together with stable cases. In the diagram,  $\langle\beta\rangle$  normalized to  $t^2$  is plotted versus  $T_e^{3/2}$ . Almost all data are bounded by the dashed line representing an empirical value for a critical “stability parameter” defined by the inverse linear growth rate  $s \propto \gamma^{-1}$ .

The edge MHD modes in LHD clearly exhibit features of resistive interchange modes. The increase of the edge mode amplitudes up to the maximum beta is not consistent with ideal mode stability and reflects the reduction of shear stabilization toward high beta (correlated with low  $S$ ). Actually, the scaling of the mode amplitudes is consistent with that predicted for linear growth rates of resistive interchange modes according to  $\gamma \propto S^{-1/3}$  (Ref. 58). This has been found in detailed studies in LHD (Refs. 32 and 59) including a comparison with CHS results.<sup>44</sup> It may be concluded that resistive interchange or ballooning modes will not be relevant for reactor-grade plasmas, in particular, if advanced physics models including two-fluid theory are taken into account.<sup>60</sup>

### III. DISCUSSION AND CONCLUSIONS

The results obtained in the high-beta regime in W7-AS and LHD are considered to be of great relevance for

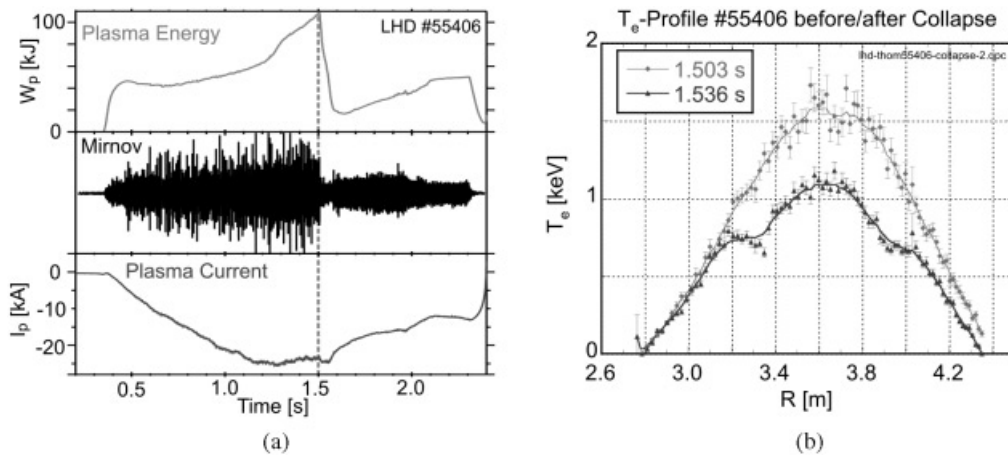


Fig. 11. Collapse of plasma energy in LHD due to an  $m/n = 1/1$  interchange mode. A small gamma parameter ( $\gamma = 1.129$ ) along with co-current generates a low-shear iota profile with  $t = 1$  in the plasma core. A flattened region in the  $T_e$  profile is formed during the collapse (right).

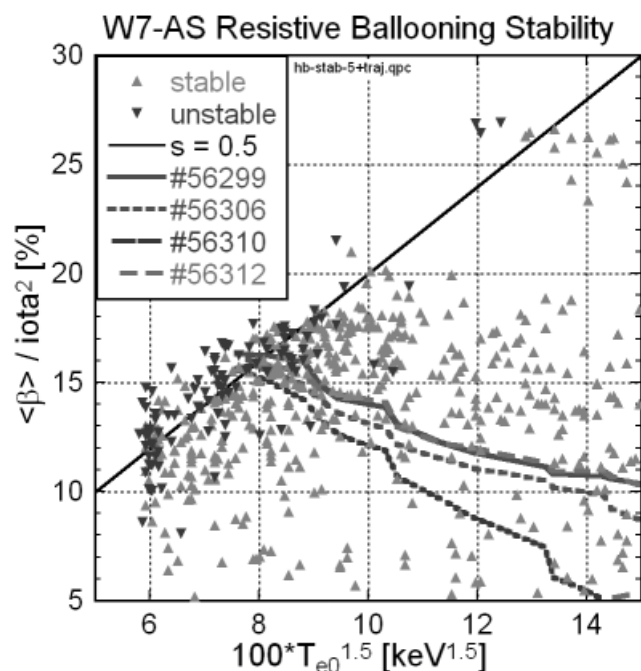


Fig. 12. Database of  $\langle \beta \rangle$  normalized to  $\iota^2$  versus  $T_e^{3/2}$  of high-beta discharges in W7-AS. The parameters just prior to MHD collapses (solid triangles) are close to a critical value of the inverse linear growth rate (dotted line “ $s = 0.5$ ”). The solid lines are the trajectories of individual discharges until the collapse.

evaluating the prospects of the future stellarator program. The two new devices presently under construction, W7-X and NCSX, are both extensively optimized with respect to confinement and MHD properties. But, they are located in totally different corners of the configuration space, and this will provide another wealth of new results.

The configuration and size of the W7-AS and LHD devices are rather different, too. However, the global confinement is comparable as follows from the comparison with common scaling laws. In order to achieve good confinement, the LHD configuration has to be optimized by exploiting the flexibility of the device, but implicating reduced stability. However, deleterious effects of MHD instabilities on the confinement in LHD have not been found so far or can be avoided, even in unstable regimes. Therefore, one might argue that configuration optimization, as partially achieved in W7-AS or more completely implemented in W7-X, may not be required to such an extent. In Helias systems (W7-X), however, a trade-off between different desired configuration properties is not necessary. The most important goals including good confinement, good equilibrium surfaces, and sufficient high MHD stability can be achieved simultaneously.

The successful test of the island divertor concept in W7-AS and the demonstration of steady-state plasma

operation in LHD using the LID head are important milestones toward power handling and exhaust control required for steady-state systems. Long-pulse experiments in LHD with moderate heating power have resulted in a pulse of 1905-s duration and a total input heating energy of 1.3 GJ exceeding the previous record by Tore Supra of 1.07 GJ. W7-X is designed to sustain heating powers up to 10 MW for 30 min. Demonstration of this capability will be another important step.

A crucial issue for each stellarator and helical device is to establish plasma core conditions with good confinement (but without impurity accumulation) compatible with steady-state operation. The HDH mode in W7-AS (Ref. 19) is a favored scenario compliant with high-beta parameters.<sup>8,9</sup> However, it remains a big issue whether this regime can be attained in W7-X since the density threshold in W7-AS is larger than the achievable densities in W7-X according to density limit scaling laws.<sup>25,26</sup> In this respect, the expectations concerning the achievable plasma beta and density are close to those in LHD.

In the high-beta regime, a convincing demonstration of steady-state power handling is still missing. The biggest issue connected to this seems to be keeping control of the edge topology as beta is increased. In the present devices, the relative large Shafranov shift, the progressive stochastization of the outer plasma region, and the change of the configuration by net toroidal current such as bootstrap and Ohkawa currents are not compatible with proper island divertor operation. External current drive by electron cyclotron waves may be a possibility to maintain current-free operation in future large devices.<sup>61,62</sup>

With respect to the Shafranov shift, the studies in W7-AS and LHD, but also in CHS (Ref. 12), have shown a good agreement with 3-D equilibrium code calculations with VMEC, HINT, and PIES. In particular, the partial optimization of the W7-AS configuration resulting in reduced Shafranov shift could be verified.<sup>8</sup> Therefore, the expected equilibrium properties for W7-X (and NCSX) seem to be reliable given the available equilibrium benchmarking. In particular, the stiffness of the W7-X configuration should ensure maintaining a sufficiently fixed profile of the rotational transform and hence a passively stable island divertor configuration.

As regards the pressure-induced destruction of magnetic surfaces, the predictions by PIES and HINT have provided more insight into the physics of the equilibrium limit. But, also, the analyses have posed new issues as to what extent plasma dynamics has to be included in the equilibrium models to make allowance for island healing effects. In connection with it, the equilibrium reconstruction in the presence of finite pressure gradients in an ergodic edge region requires additional effort. Nevertheless, the PIES calculations for W7-X (Ref. 63) and NCSX (Ref. 4) give much better results in the high-beta regime. This is achieved in W7-X by the significant reduction of the Pfirsch-Schlüter current and the optimized coil field

spectrum. In NCSX, a particular “coil healing” procedure is applied to compensate contributions due to equilibrium currents by those of resonant coil perturbations.<sup>64,65</sup> Therefore, a sufficiently high quality of finite-beta flux surfaces may be expected in W7-X and in NCSX as well.

Also, the effect of net currents on the edge topology is considered to pose no big problem in W7-X. An important goal was to eliminate the bootstrap current along with the reduction of the Pfirsch-Schlüter current in order to keep passive control of the magnetic configuration. This is of course quite different than in NCSX, where bootstrap current drive is an essential element of the QAS approach. The generation and control of substantial plasma current and the maintenance of kink stability in NCSX impose greater shape control requirements than in previous stellarators. NCSX is a proof-of-principle experiment that has to demonstrate a novel physical concept and its technical realization. The challenge for the future will be to incorporate the features required for reactor capability, i.e., to develop a compatible power exhaust system and to minimize active configuration control.

Concerning MHD stability an important result consists of the absence of fast disruptive instabilities even close to operational limits determined by equilibrium deterioration, density limit, or confinement (power). The plasma reaction mostly occurs via slow transitions to increased transport. This is an important advantage compared with tokamak devices where disruptions usually inhibit the approach or exceeding of operational limits. Although the local ideal MHD stability seems to underestimate the stability found in W7-AS and LHD experiments, the linearized ideal MHD analyses are still useful. The observed mode activity, even if not always relevant for confinement, is mostly correlated with the predicted unstable regions. An important nonlinear effect could be mode saturation on a low level due to local pressure profile flattening.<sup>66</sup> The data suggest that relevant MHD modes are absent, if Mercier stability is ensured. Another important finding at LHD is the identification of “confinement relevant” modes correlated with ideal low- $n$  interchange modes of a sufficiently large growth rate and radial width ( $\geq 5\%$  of plasma radius). These modes provide a good estimate of an ideal stability limit that cannot be exceeded in LHD. A stability index based on the critical width of MHD modes may provide a useful criterion to assess relevant MHD limits and to optimize stellarator configurations.

Given these results, the prospects for MHD stability in W7-X are very promising, allowing one to achieve stable high-beta plasma operation. NCSX has to face more efforts to achieve a stationary current profile and to control the iota profile and plasma shape during the path to high beta. The LHD device has reached the record of  $\langle \beta \rangle \geq 4\%$  in stellarators and helical devices without being limited by deleterious MHD instabilities. However, the

requirements with respect to equilibrium (low Shafranov shift) and stability (sufficient magnetic well depth), as well as with respect to confinement (favorable inwardly shifted configuration) and stability (favorable outward shift) are conflicting. Also, the magnetic hill region with large magnetic shear may be susceptible not only to resistive but also to ideal interchange modes at higher beta and to field stochasticization. More detailed studies of the stability limit in LHD seem to be feasible if higher heating power is available.

Another remaining issue in the future stellarator program, not discussed so far, is Alfvén and fishbone instabilities excited by resonances with energetic particles. Besides the modes well known from tokamak research, stellarator Alfvén eigenmodes such as helicity-induced or mirror-induced Alfvén eigenmodes have been predicted<sup>47,67,68</sup> and found in the W7-AS and LHD experiments.<sup>8,40,42,69</sup> Usually, they do not play an important role under the present high-beta conditions because the fraction of resonant fast injected ions is relatively small. However, Alfvén modes may be of great relevance in reactorlike plasmas.

It seems to be very important in future experimental devices to provide sufficient flexibility for changing and controlling the magnetic configuration. This will be realized to a large extent in W7-X and NCSX. External current drive capability should be available depending on the magnitude of the bootstrap and NBI currents appearing in experiment. Also, advanced diagnostic systems are required to obtain reliable reconstructions of the equilibrium profiles. Together with the development of more sophisticated physics MHD models, this will allow one to prepare a good physics basis for a stellarator fusion reactor.

## REFERENCES

1. ITER TEAMS, *Nucl. Fusion*, **36**, 2137 (1999).
2. J. NÜHRENBERG and R. ZILLE, “Stable Stellarators with Medium  $\beta$  and Aspect Ratio,” *Phys. Lett. A*, **114**, 129 (1986).
3. S. P. HIRSHMAN et al., “Physics of Compact Stellarators,” *Phys. Plasmas*, **6**, 1858 (1999).
4. M. C. ZARNSTORFF et al., “Physics of the Compact Advanced Stellarator NCSX,” *Plasma Phys. Control. Fusion*, **43**, A237 (2001).
5. F. S. B. ANDERSON et al., “The Helically Symmetric Experiment (HSX) Goals, Design and Status,” *Fusion Technol.*, **27**, 273 (1995).
6. O. MOTOJIMA et al., “Confinement and MHD Stability in the Large Helical Device,” *Proc. 21st IAEA Fusion Energy Conf.*, Vilamoura, Portugal, November 1–6, 2004, EX/3-4, OV1-4, International Atomic Energy Agency (2004).

7. H. YAMADA et al., "Configuration Flexibility and Extended Regimes in Large Helical Device," *Plasma Phys. Control. Fusion*, **43**, A55 (2001).
8. A. WELLER et al., "Experiments Close to the Beta-Limit in W7-AS," *Plasma Phys. Control. Fusion*, **45** A285 (2003).
9. M. C. ZARNSTORFF et al., "Equilibrium and Stability of High-Beta Plasmas in Wendelstein 7-AS," *Proc. 21st IAEA Fusion Energy Conf.*, Vilamoura, Portugal, November 1–6, 2004, EX/3–4, International Atomic Energy Agency (2004).
10. M. WAKATANI and S. SUDO, "Overview of Heliotron-E Results," *Plasma Phys. Control. Fusion*, **38**, 933 (1996).
11. J. H. HARRIS et al., "Second Stability in the ATF Torsatron," *Phys. Rev. Lett.*, **63**, 1249 (1989).
12. S. OKAMURA et al., "High Beta Discharges with Neutral Beam Injection in CHS," *Nucl. Fusion*, **35**, 283 (1995).
13. H. RENNER et al., "Initial Operation of the Wendelstein 7AS Advanced Stellarator," *Plasma Phys. Control. Fusion*, **31**, 1579 (1989).
14. F. WAGNER et al., "W7-AS: One Step of the Wendelstein Stellarator Line," *Phys. Plasmas*, **12**, 072509 (2005).
15. P. GRIGULL et al., "First Island Divertor Experiments on the W7-AS Stellarator," *Plasma Phys. Control. Fusion*, **43**, A175 (2001).
16. A. IYOSHI et al., "Overview of the Large Helical Device Project," *Nucl. Fusion*, **39**, 1245 (1999).
17. N. OHYABU et al., "Bifurcation of Equilibria Between With and Without a Large Island in the Large Helical Device," *Plasma Phys. Control. Fusion*, **47**, 1431 (2005).
18. S. P. HIRSHMAN et al., "Improved Radial Differencing for Three-Dimensional Magnetohydrodynamic Equilibrium Calculations," *J. Comput. Phys.*, **87**, 396 (1990).
19. K. McCORMICK et al., "New Advanced Operational Regime on the W7-AS Stellarator," *Phys. Rev. Lett.*, **89**, 015001-1 (2002).
20. O. MOTOJIMA et al., "Recent Advances in the LHD Experiment," *Nucl. Fusion*, **43**, 1674 (2003).
21. U. STROTH et al., "Energy Confinement Scaling from the International Stellarator Database," *Nucl. Fusion*, **36**, 1063 (1996).
22. J. MIYAZAWA et al., "Temperature Dependence of the Thermal Diffusivity in High-Collisionality Regimes in the Large Helical Device," *Plasma Phys. Control. Fusion*, **47**, 801 (2005).
23. N. A. UCKAN, "ITER Physics Design Guidelines," p. 10, International Atomic Energy Agency (1990).
24. H. YAMADA et al., "Characterization of Edge Pressure in the Large Helical Device," *Plasma Phys. Control. Fusion*, **44**, A245 (2002).
25. S. SUDO et al., "Scalings of Energy Confinement and Density Limit in Stellarator/Heliotron Devices," *Nucl. Fusion*, **30**, 11 (1990).
26. L. GIANNONE et al., "Radiation Power Profiles and Density Limit with a Divertor in the W7-AS Stellarator," *Plasma Phys. Control. Fusion*, **44**, 2149 (2002).
27. H. WOBIG, "The Theoretical Basis of a Drift-Optimized Stellarator Reactor," *Plasma Phys. Control. Fusion*, **35**, 903 (1993).
28. K. Y. WATANABE et al., "Progress of High-Beta Experiments in Stellarator/Heliotron," *Fusion Sci. Technol.*, **46**, 24 (2004).
29. T. KOBUCHI et al., "Shafranov Shift Measurement Using Soft X-Ray CCD Camera on Large Helical Device," *Europhysics Conference Abstracts: 31st Conf. Plasma Physics*, London, United Kingdom, June 28–July 2, 2004, Vol. 28B, p. P-5.115, European Physical Society (2004).
30. K. HARAFUJI, T. HAYASHI, and T. SATO, "Computational Study of Three-Dimensional Magnetohydrodynamic Equilibria in Toroidal Helical Systems," *J. Comput. Phys.*, **81**, 169 (1989).
31. A. H. REIMAN and H. GREENSIDE, "Numerical Solution of Three-Dimensional Magnetic Differential Equations," *J. Comput. Phys.*, **75**, 423 (1988).
32. K. Y. WATANABE and S. SAKAKIBARA, "Subjects on MHD Equilibrium in the LHD Experiments," presented at U.S.-Japan JIFT Workshop, Kyoto, Japan, January 25–27, 2005.
33. K. Y. WATANABE, "Effects of Configuration on Transport and MHD Phenomena," presented at Magnetohydrodynamics Mtg. Magnetic Field Structure and Improvement of MHD Stability by Pressure Profile Control, February 18, 2005, Toki-shi, Japan.
34. Y. NAGAYAMA et al., "Experiment of Magnetic Island Formation in Large Helical Device," *Nucl. Fusion*, **45**, 888 (2005).
35. R. KANNO et al., "Formation and Healing of  $n = 1$  Magnetic Islands in LHD Equilibrium," *Nucl. Fusion*, **45**, 888 (2005).
36. K. ITOH, S.-I. ITOH, and M. YAGI, "Self-Sustained Annihilation of Magnetic Islands in Helical Plasmas," *Phys. Plasmas*, **12**, 072512 (2005).
37. M. C. ZARNSTORFF et al., "The Saturation of Beta in W7-AS," *Europhysics Conference Abstracts: 32nd Conf. Plasma Physics*, Tarragona, Spain, June 27–July 1, 2005, Vol. 29C, p. P-1.062, European Physical Society (2005).
38. N. NAKAJIMA et al., "Boundary Modulation Effects on MHD Instabilities in Heliotrons," *Proc. 21st IAEA Fusion Energy Conf.*, Vilamoura, Portugal, November 1–6, 2004, TH5-6, International Atomic Energy Agency (2004).
39. M. FUJIWARA et al., "Overview of LHD Experiments," *Nucl. Fusion*, **41**, 1355 (2001).

40. A. WELLER et al., "Survey of Magnetohydrodynamic Instabilities in the Advanced Stellarator Wendelstein 7-AS," *Phys. Plasmas*, **9**, 931 (2001).
41. S. SAKAKIBARA et al., "Effect of MHD Activities on Pressure Profile in High- $\beta$  Plasmas of LHD," *Plasma Phys. Control. Fusion*, **44**, A217 (2002).
42. K. TOI et al., "MHD Instabilities and Their Effects on Plasma Confinement in Large Helical Device Plasmas," *Nucl. Fusion*, **44**, 217 (2004).
43. S. SAKAKIBARA et al., "MHD Activities in High-Regime of LHD," *Europhysics Conference Abstracts: 31st Conf. Plasma Physics*, London, United Kingdom, June 28–July 2, 2004, Vol. 28G, p. O-4.01 (2004).
44. S. SAKAKIBARA et al., "MHD Characteristics in the High Beta Regime of the Large Helical Device," *Nucl. Fusion*, **41**, 1177 (2001).
45. K. Y. WATANABE et al., "Effects of Global MHD Instability on Operational High Beta-Regime in LHD," *Nucl. Fusion*, **45**, 1247 (2005).
46. C. SCHWAB, "Ideal Magnetohydrodynamics: Global Mode Analysis of Three-Dimensional Plasma Configurations," *Phys. Fluids B*, **5**, 3195 (1993).
47. C. NÜHRENBERG, "Compressional Ideal Magnetohydrodynamics: Unstable Global Modes, Stable Spectra, and Alfvén Eigenmodes in Wendelstein 7-X-Type Equilibria," *Phys. Plasmas*, **6**, 137 (1999).
48. A. KOMORI et al., "Recent Results from the Large Helical Device," *Plasma Phys. Control. Fusion*, **45**, 671 (2003).
49. K. Y. WATANABE et al., "Relationships Between the Prediction of Linear MHD Stability Criteria and the Experiment in LHD," *J. Plasma Fusion Res. Ser.*, **6**, 523 (2004).
50. K. ICHIGUCHI et al., "Effects of Net Toroidal Current Profile on the Mercier Criterion in Heliotron Plasmas," *Nucl. Fusion*, **42**, 557 (2002).
51. W. A. COOPER, "Variational Formulation of the Linear MHD Stability on 3D Plasmas with Noninteracting Hot Electrons," *Plasma Phys. Control. Fusion*, **34**, 1011 (1992).
52. S. OHDACHI, "Internal Disruptions Observed by the High Speed Tangentially Viewing Soft X-Ray Camera," presented at Magnetohydrodynamics Mtg. Magnetic Field Structure and Improvement of MHD Stability by Pressure Profile Control, February 18, 2005, Toki-shi, Japan.
53. A. WELLER et al., "MHD Effects Related to High-Beta Operation in WENDELSTEIN W7-AS," *Europhysics Conference Abstracts: 32nd Conf. Plasma Physics*, Tarragona, Spain, June 27–July 1, 2005, Vol. 29C, p. P-4.056, European Physical Society (2005).
54. K. MIYAMOTO, *Plasma Physics for Nuclear Fusion*, MIT Press (1980).
55. G. BATEMAN and D. B. NELSON, "Resistive-Ballooning-Mode Equation," *Phys. Rev. Lett.*, **41**, 1805 (1978).
56. R. SÁNCHEZ et al., "Compressibility Effects on Ideal and Resistive Ballooning Stability in the TJ-II Heliac Device," *Nucl. Fusion*, **37**, 1363 (1997).
57. R. KAISER, "Resistive Ballooning Modes in W7-AS and W7-X," *Nucl. Fusion*, **33**, 1281 (1993).
58. K. ICHIGUCHI et al., "Ideal and Resistive Pressure Gradient Driven Instabilities in Heliotron DR," *Nucl. Fusion*, **29**, 2093 (1989).
59. S. SAKAKIBARA et al., "Recent Progress of MHD Study in High- $\beta$  Plasmas of LHD," *Proc. 15th Int. Stellarator Workshop*, Madrid, Spain, October 3–7, 2005, p. IT-07 (2005).
60. H. R. STRAUSS et al., "Simulation of Two Fluid and Energetic Particle Effects in Stellarators," *Nucl. Fusion*, **44**, 1008 (2004).
61. Yu. TURKIN et al., "Current Control by ECCD for W7-X," *Proc. 15th Int. Stellarator Workshop*, Madrid, Spain, October 3–7, 2005, p. OT-10 (2005).
62. S. FERRANDO I MARGALET et al., "Electron Cyclotron Current Drive Compensation of the Bootstrap Current in Quasi-Symmetric Reactor Devices," *Proc. 15th Int. Stellarator Workshop*, Madrid, Spain, October 3–7, 2005, p. P1-27 (2005).
63. M. DREVLAK et al., "PIES Free Boundary Stellarator Equilibria with Improved Initial Conditions," *Nucl. Fusion*, **45**, 731 (2005).
64. S. R. HUDSON et al., "Free-Boundary Full-Pressure Island Healing in Stellarator Equilibria: Coil-Healing," *Plasma Phys. Control. Fusion*, **44**, 1377 (2002).
65. S. R. HUDSON et al., "Constructing Integrable High-Pressure Full-Current Free-Boundary Stellarator Magnetohydrodynamic Equilibrium Solutions," *Nucl. Fusion*, **43**, 1040 (2003).
66. K. ICHIGUCHI et al., "Nonlinear MHD Analysis for LHD Plasmas," *Nucl. Fusion*, **43**, 1101 (2003).
67. N. NAKAJIMA et al., "High- $n$  Helicity-Induced Shear Alfvén Eigenmodes," *Phys. Fluids B*, **4**, 1115 (1992).
68. Ya. I. KOLESNICHENKO et al., "Alfvén Continuum and High-Frequency Eigenmodes in Optimized Stellarators," *Phys. Plasmas*, **8**, 491 (2001).
69. K. TOI et al., "Energetic Ion Driven Alfvén Eigenmodes in Large Helical Device Plasmas with Three-Dimensional Magnetic Structure and Their Impact on Energetic Ion Transport," *Plasma Phys. Control. Fusion*, **46**, S1 (2004).